Denmark Strait overflow for Last Glacial Maximum to Holocene conditions

Frank Kösters
Institut für Geowissenschaften, Universität Kiel, Kiel, Germany

Rolf Käse
Institut für Meereskunde, Universität Hamburg, Hamburg, Germany

Kevin Fleming and Detlef Wolf
GeoForschungsZentrum Potsdam, Potsdam, Germany

Received 7 October 2003; revised 16 March 2004; accepted 22 April 2004; published 15 June 2004.

[1] The Denmark Strait plays an important role as a dense water gateway between the Arctic and the subpolar North Atlantic. Previous studies have shown that the volume transport over the sill is limited by hydraulic constraints. A regional ocean-circulation model (ROMS) with a horizontal resolution of ≈1/20° degree and 30 sigma layers in the vertical is applied to study the through flow characteristics for Last Glacial Maximum to Holocene conditions. The bathymetry of the gateway region is obtained from a geodynamic model that takes into account the differential ice loading of the adjacent continents. First, the upstream reservoir conditions are systematically changed to test hydraulic limitations for altered bathymetry. Generally, the through flow is less than the predicted maximal value from hydraulic theory by almost 50%. The results indicate that the reduction in gateway depth and aperture owing to glacial-isostatic processes alone lead to a considerable further reduction of the overflow, by approximately 33%, compared to the present day. Second, the through flow is modeled using average density profiles and wind stress from global model data. The reduction in the density-driven part of the overflow is partly compensated by an enhanced wind stress but is still reduced by a factor of 5. Owing to the narrowing of the strait during the glacial and the increased northerly wind, the North Icelandic Irminger Current was strongly reduced but still existent. *INDEX TERMS:* 1635 Global Change: Oceans (4203); 4255 Oceanography: General: Numerical modeling; 4267 Oceanography: General: Paleoceanography; 4556 Oceanography: Physical: Sea level variations; *KEYWORDS:* overflow, Denmark Strait, hydraulic control

Citation: Kösters, F., R. Käse, K. Fleming, and D. Wolf (2004), Denmark Strait overflow for Last Glacial Maximum to Holocene conditions, *Paleoceanography*, *19*, PA2019, doi:10.1029/2003PA000972.

1. Introduction

[2] The Denmark Strait Overflow plays a major role as a dense water gateway between the Nordic Seas and the North Atlantic under present-day climate conditions [*Hansen and Østerhus*, 2000]. Dense water formed in the Nordic Seas flows over the Greenland Scotland Ridge and enters the North Atlantic to contribute to the North Atlantic Deep Water. Volume transport, variability and the path of the overflow have already been previously studied. *Saunders* [2001] found (even though the transport shows variability over short timescales of up to 10 days) the mean to remain fairly constant over time. Seasonal variations have not been detected so far in measurements [*Dickson et al.*, 2002] but there is evidence for a correlation between transport and the North Atlantic Oscillation [*Blindheim et al.*, 2000]. However, the mean transport appears to be limited by hydraulic constraints [*Whitehead*, 1998], an observation supported by numerical modeling [*Käse and Oschlies*, 2000]. The validity of hydraulic theory as demonstrated for present-day conditions with numerical models and observations [*Girton et al.*, 2001; *Nikolopoulos et al.*, 2003] has given rise to the question as to whether this is also a useful tool for studying the Denmark Strait Overflow (DSO) for different climatic conditions, e.g., the Last Glacial Maximum. In case of the Mediterranean outflow, hydraulic constraints on maximum overflow strength based on hydrography and bathymetry have been successfully demonstrated [*Matthiesen and Haines*, 2003].

[3] It is still a point of debate whether the DSO played a similarly important role in deep water formation during the last 21 kyr as it does today [e.g., *Sarnthein et al.*, 2001]. For present-day conditions, the overflow of dense water over the Greenland-Scotland Ridge is more important for the water budget than wind-driven surface outflows [*Hansen and Østerhus*, 2000]. Considering Last Glacial Maximum (LGM) conditions, there are no direct transport estimates. From the lithofacies and chronology of sediment cores at the southern end of the Denmark Strait an indirect measure of overflow strength can be obtained suggesting that the overflow had its present strength from around 12 ka BP

0883-8305/04/2003PA000972

[*Völker*, 1999; *Andrews and Cartee-Schoolfield*, 2003]. Commonly, $\delta^{13}C$ values are used as ventilation proxies for identifying water masses [*Elliot et al.*, 2002; *Curry et al.*, 1988], and the overflow strength is inferred from these. *Hagen and Hald* [2002] developed a new $\delta^{18}O$ versus $\delta^{13}C$ proxy which allows to reconstruct the glacial water masses and the deep water formation processes. In many paleoceanographic studies the focus is on the millennial-scale variability reflected in $\delta^{18}O$ values from foraminifera found in sediment cores. *van Kreveld et al.* [2000] suggested a correlation to the climatic records from the GISP2 ice core [*Grootes and Stuiver*, 1997] and an influence of the Denmark Strait on the pacing of Dansgaard-Oeschger (D-O) cycles.

[4] These paleoceanographic evidences show that rather small gateways as the Denmark Strait can be seen as key regions having an climatic impact on much larger regions. This is supported by evidence from numerical model studies showing that overflow processes have a significant effect on the meridional overturning circulation [*Willebrand et al.*, 2001]. Moreover, even though coarse-resolution numerical models of the glacial North Atlantic compare well with proxy data [*Paul and Schäfer-Neth*, 2003; *Meissner et al.*, 2003], the Denmark Strait is not properly resolved in these models and hence transport estimates are not reliable.

[5] Therefore the two main objectives of this study are (1) to determine the maximal hydraulically controlled flow through Denmark Strait for realistic bathymetries since the last glacial (present day (0 ka BP), deglacial (11.3 ka BP) and LGM (21.5 ka BP)) and (2) to obtain realistic transports for the present day and the LGM in order to assess water mass pathways and faunal exchanges. We use a high-resolution numerical model to (1) determine the transport through Denmark Strait for an idealized density field. The results from the numerical model are then compared to transport limitations obtained from hydraulic theory. Whereas in (2) average density profiles and wind stress are applied to compare present-day winter and LGM summer conditions to obtain realistic transport estimates and pathways.

2. Background: Marine Geology and Oceanography

2.1. Denmark Strait Bathymetry

[6] The model bathymetry is important for the hydraulically controlled flow investigated here. For present-day conditions, it is provided at a high resolution of 5' from ETOPO5 [*National Center for Atmospheric Research* (*NCAR*), 1986] (Figure 1a). The LGM bathymetry can be estimated from the present-day bathymetry by accounting for eustatic sea level change. *Clark and Mix* [2002] reviewed different estimates for the LGM sea level lowering and found a range from 118 m to 130 m based on ice-

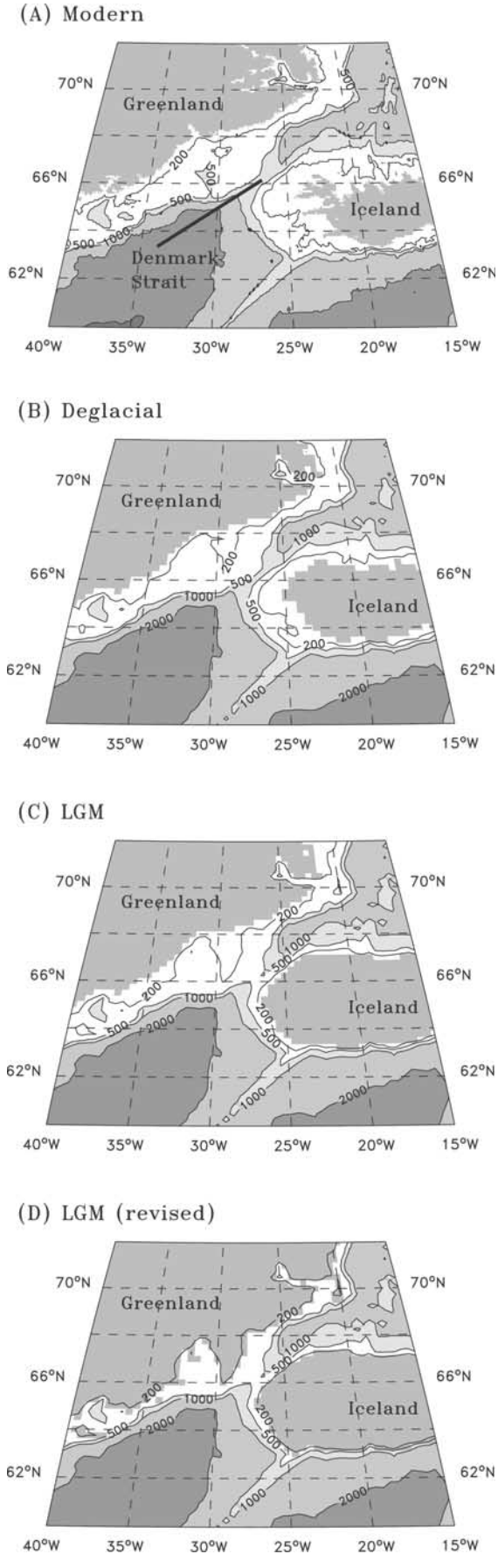

Figure 1. Bathymetry of Denmark Strait for (a) the present (0 ka BP), (b) the glacial-interglacial transition (11.3 ka BP) and (c and d) the Last Glacial Maximum (21.5 ka BP). Bathymetries (Figures 1b, 1c, and 1d) are based on the GIA models. Figure 1c is the favored model of *Fleming and Lambeck* [2004] while Figure 1d includes a more extensive and possibly more realistic ice extend.

dynamic reconstructions that are in accordance with the CLIMAP minimum model of 127.5 m. A global sea level lowering of 120 m for the LGM is commonly used. Changes in bathymetry are also due to the advance and retreat of the land-based ice sheets and the accompanying isostatic rebound. The contribution of glacial-isostatic adjustment (GIA) to changes in the bathymetry of the Denmark Strait is found using a numerical model developed at the Research School of Earth Sciences, the Australian National University [e.g., *Lambeck et al.*, 1998]. The ice models employed have been constrained using geological evidence, especially relative sea level data. Geological evidence points toward glaciated shelves between Greenland and Iceland, even though the maximum extent remains uncertain. Seismic sections detect the greatest extent of the ice sheet off the SE Greenland shelf [*Larsen*, 1983], with the depth of grounded ice extending to 200 m to 400 m below present-day sea level. However, it is not certain if this extension is related to the last glaciation or the previous one. Using carbonate accumulation rates and seafloor properties, *Mienert et al.* [1992] developed a qualitative model that indicates an almost fully glaciated shelf. For an improved chronology of the ice sheet extent, better time control is necessary, which may be obtained using ^{14}C dates of marine and terrestrial biotopes [e.g., *Funder and Hansen*, 1996]. They found that the extension of the ice margin was roughly at the 300 m depth isobath of present-day bathymetry, suggesting that ~70% of the shelf was ice covered during the LGM. Their reconstruction indicates a distance of only 150 km between the ice sheets of Iceland and Greenland. However, this estimate may be too conservative since the oldest shells found on the shelf were formed at 17 ka BP [*Bennike and Björck*, 2002], suggesting a fully glaciated shelf during the LGM. From ice-dynamic modeling, *Huybrechts* [2002] found that the Greenland Ice Sheet may have extended beyond the present-day coast line between 25 and 15 ka BP. By 10 ka BP, the ice sheet had retreated close to the current coastline and was approximately at the current ice margin at 4.5 ka BP. The GIA mentioned earlier was used to determine changes in the Denmark Strait's bathymetry [*Fleming and Lambeck*, 2004] and provided data for the LGM (21.5 ka BP) and the glacial-interglacial transition (11.3 ka BP) (Figures 1b and 1c).

[7] The geodynamic model combines eustatic and glacial isostatic effects resulting from fluctuations in the global ice regime. Since a GIA model that accommodates lateral variations in Earth's rheology parameter values was unavailable to us, we first determined the GIA response from the land-based ice sheets, excluding Iceland, using a global average earth model, and then added the response from Iceland that was found separately using a more realistic structure for that area. The Greenland ice model is from *Fleming and Lambeck* [2004] and was derived from the minimum and maximum ice sheets of *Denton and Hughes* [1981]. The Iceland model was from the maximum of *Denton and Hughes* [1981] with timing from *Ingolfsson et al.* [1994]. Using these models, we found that the LGM sill depth was ~509 m compared to 581 m for the present. Although the LGM model underestimates the extent of the ice sheet slightly, the overall agreement between the geodynamic model and geological field studies is satisfactory. In order to test the sensitivity of our results to the lateral extension of the ice sheet, we used an additional bathymetry (Figure 1d) where the extent was increased to match the reconstruction of *Funder and Hansen* [1996].

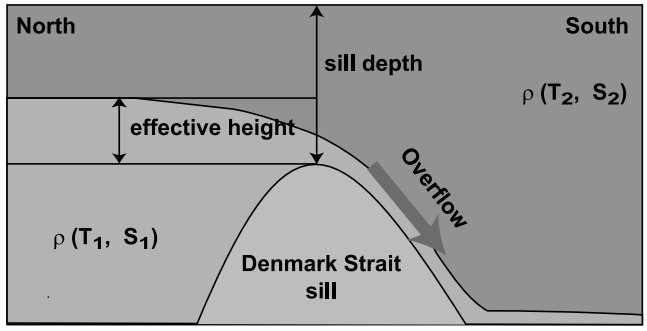

Figure 2. Schematic overflow model. Illustrating the parameters effective height H_{eff}, the density contrast ($\Delta\rho = \rho(T_2, S_2) - \rho(T_1, S_1)$), and the sill depth used in the text.

2.2. Oceanography of the Denmark Strait

[8] The time-mean large-scale circulation north of the Greenland-Scotland Ridge follows mainly closed contours of f/H, the Coriolis parameter f over water depth H [*Nost and Isachsen*, 2003]. However, through the Denmark Strait and the Faroe Bank Channel, the two most important gaps in the Greenland-Scotland Ridge, dense water is spilled into the North Atlantic and contributes to the formation of North Atlantic Deep Water. This process affects the global meridional overturning for the present day [*Willebrand et al.*, 2001] and the last glacial [*Sarnthein et al.*, 2001]. It has been shown that for present-day conditions the amount of dense water transported through the Denmark Strait is limited by hydraulic constraints [e.g., *Käse et al.*, 2003]. As a consequence, the through flow is only depending on the average density difference across the sill $\Delta\rho$ and the height of the dense reservoir H_{eff}. In case of the Denmark Strait the flow is restricted by sidewall and bottom constrictions (Figure 1). Furthermore the average density structure [e.g., *Levitus et al.*, 1994; *Levitus and Boyer*, 1994] across the Denmark Strait resembles that of a two-layer system with a lighter layer on top of a heavier one (Figure 2).

[9] Assuming now that the upper layer is stagnant and only the lower layer moves, which is called $1^1/_2$ layer reduced gravity model, allows to describe the volume transport using rotating hydraulic theory [*Whitehead et al.*, 1974]. The flow through a constriction is hydraulically controlled when the transport is completely determined by the upstream conditions. Applied to the Denmark Strait, the magnitude of the DSO is set by the conditions in the Iceland Sea independent of mixing processes when entering the Irminger Basin. For hydraulic control to be important, the information-propagation speed, here gravity wave speed $c = \sqrt{g'H}$, with g' as the reduced gravity $g' = g\Delta\rho/\rho$ and ρ the mean density, H the layer thickness, should be comparable to the fluid advection speed u. Note that H refers to the full layer thickness (e.g., shaded area of $\rho(T_1, S_1)$ in Figure 2),

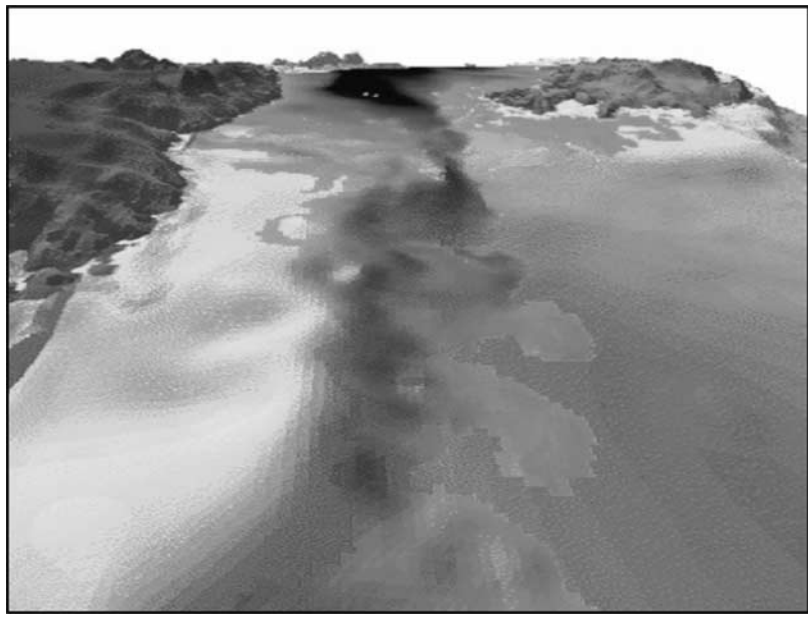

Figure 3. Snapshot of the descending overflow plume from the model experiments. Greenland is at the left, Iceland at the right margin. The shading of the overflow plume indicates the overflow thickness, with increasing thickness as darker gray and the full reservoir, as black, in the north. See color version of this figure at back of this issue.

whereas H_{eff} corresponds that part of the layer exceeding the sill height (effective height in Figure 2). Then information cannot travel back upstream and the flow is independent of downstream conditions. For the Denmark Strait today with typical values of $c = \sqrt{0.0033\,\mathrm{m\,s^{-2}} \cdot 157\,\mathrm{m}} = 0.72$ m/s and observed velocities at the sill of up to 1.3 m/s and a mean velocity of 0.56 m/s [*Girton and Sanford*, 2003] the flow is hydraulically controlled. In climate models, however, u = O(0.1 m/s), while c is relatively unchanged. Therefore the flow is not hydraulically controlled and does not represent the physical mechanisms properly. F. Kösters (Denmark Strait overflow: Comparing model results and hydraulic transport estimates, submitted to *Journal of Geophysical Research*, 2004, hereinafter referred to as Kösters, submitted manuscript, 2004) compared different theoretical transport calculations and suggested the method of *Whitehead et al.* [1974] is most applicable for paleoceanographic questions. *Whitehead et al.* [1974] showed that for a fixed sill depth the transport is limited to

$$Q = \frac{1}{2}\frac{g' H_{eff}^2}{f}. \qquad (1)$$

Equation (1) is the special case of wide sills, where the characteristic length scale, here the sill width L = 350 km, is large compared to baroclinic Rossby radius (mean eddy size), here 14 km. The hydraulic transport limitation is an upper bound on the transport, which is probably reduced by effects not considered in this theory such as friction.

3. Numerical Model for the Overflow Region

[10] The experiments were carried out with the Regional Ocean Modeling System (ROMS) [*Haidvogel et al.*, 2000; *Shchepetkin and McWilliams*, 2004] using two different setups, one focused on the Denmark Strait (experiment DS in the following) as in the work of Kösters (submitted manuscript, 2004) and the other including the full Greenland-Scotland Ridge (experiment GSR henceforth). The experimental setups are very similar but differ in lateral extent mainly therefore only experiment DS is here briefly explained and experiment GSR only if different from DS.

[11] The Denmark Strait was investigated using 30 equally spaced, topography following (sigma coordinate) layers in the vertical and a fixed horizontal resolution of ≈1/20° (Figure 3).

[12] The topography was smoothed for numerical reasons [*Haidvogel and Beckmann*, 1999], but the characteristic values for the Denmark Strait are kept at a depth of 580 m and a width of 350 km. In DS the density structure was simplified and it was assumed that density ρ depends on potential temperature θ alone, according to the linear equation of state. The model was initialized with two water masses having a potential temperature (density) of θ = −1°C (σ_θ = 28.08) north of the sill and θ = +5°C (σ_θ = 27.60) south of the sill, resembling the average two respective temperatures. For transport calculations a passive tracer initially distributed just north of the sill is used. Calculating the transport from the passive tracer should give the most unbiased estimate since no DSOW definition is needed. The model was integrated for 60 days, when a quasi-steady state was reached and days 20 to 60 were analyzed.

[13] In GSR, mean temperature and salinity profiles were employed hence better representing the effects of stratification. These profiles were restored at the northern and southern boundary as lateral forcing. In addition to this buoyancy forcing we used a mean wind stress to force the model. The present-day experiments are representing mean

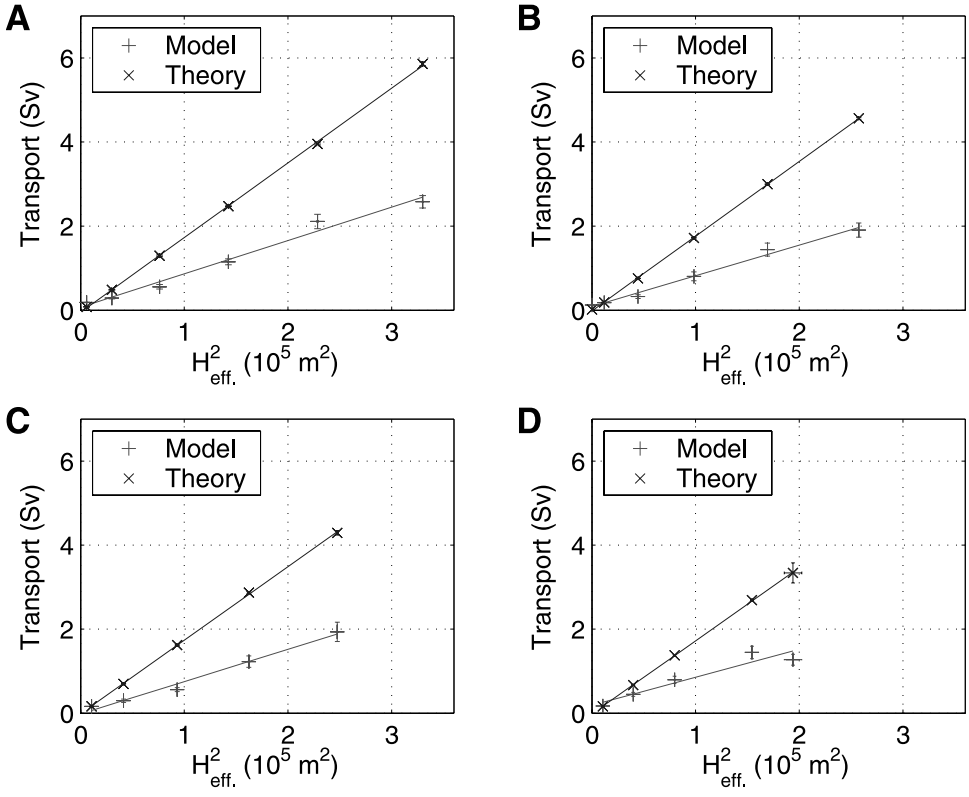

Figure 4. (a–d) Dense water transport as a function of squared effective height for experiments DS A-D.

winter conditions whereas the LGM run resembles a mean summer (JJA) situation. Owing to differences in the model setup and the larger domain we had to integrate the model for 60 days to reach equilibrium and then analyzed days 90 to 130.

4. Hydraulic Transport

[14] The experiments DS focus on the effects of topography changes on the modeled and theoretical transport. First, we will briefly discuss results from the reference run (Kösters, submitted manuscript, 2004) using the present-day bathymetry. Second, the relation of reservoir height to transport will be discussed for glacial and deglacial conditions. Third, the dependence of transport on density contrast is used to assess the paleo-overflow strength. The theoretical transport is calculated from the mean upstream effective height and the mean density difference upstream versus downstream. As pointed out by Kösters (submitted manuscript, 2004), this does not give the best fit to the transport in terms of reflecting variability, but provides a robust estimate of the mean transport. We have decided to use this simplified method in order to provide a template to calculate transport from sparse information, such as the geological record, or coarse information, such as from GCMs.

4.1. Experiment DS

[15] To establish a relation between transport Q and effective height H_{eff} the thickness of the warm layer on top of the cold reservoir was changed systematically from 0 m to 500 m in steps of 100 m for four bathymetries resembling the conditions at present day (0 ka BP), glacial-interglacial transition (11.3 ka BP) and LGM A/B (21.5 ka BP). The transport is plotted versus the squared effective height in order to better show the assumed quadratic relation ($Q \propto H^2_{eff}$). From Figure 4 one can see that the theoretical transport provides an upper limit on the modeled transport for all experiments.

[16] The expected quadratic relation of effective height and transport shows high correlation and a mean ratio of modeled to theoretical transport of 0.46 ± 0.15 for all experiments (Table 1).

[17] The theoretical limit can be linearly scaled down to give a best fit on the modeled transport, which then allows to predict the transport from the effective height and density contrast only. It should be pointed out that, in Figure 4, transport is plotted against reservoir height. Owing to the reduced sill depth for the LGM the cold water interface must be higher to achieve the same reservoir height (com-

Table 1. Summary for Experiments DS A-D With Varying Effective Height

Experiment	Time Slice, kyr BP	Ratio Model/Theory	Correlation R^2
DS A	0	0.47	0.98
DS B	11.4	0.44	0.99
DS C	21.5	0.44	0.99
DS D	21.5	0.47	0.91

pare Figure 2). Hence, for the same density profile, the upper LGM transport limit is reduced by 33% due to the decrease in sill depth from 581 m to 509 m using the observed present-day effective height of 400 m. The geodynamic model for the glacial transition (11.3 ka BP) results in a similar sill depth (513 m) as for the LGM (509 m), therefore the biggest differences are restricted to the shelf. This implies that the overflow was still reduced by 31% due to topography during this time. An important result is that the same relationship is valid for different bathymetries. For each bathymetry, a scaling factor can be found to predict transport from reservoir height. Moreover, the differences in these scaling factors between the experiments are small, suggesting that an average value of 0.5 ± 0.2 can be used over the geological times considered.

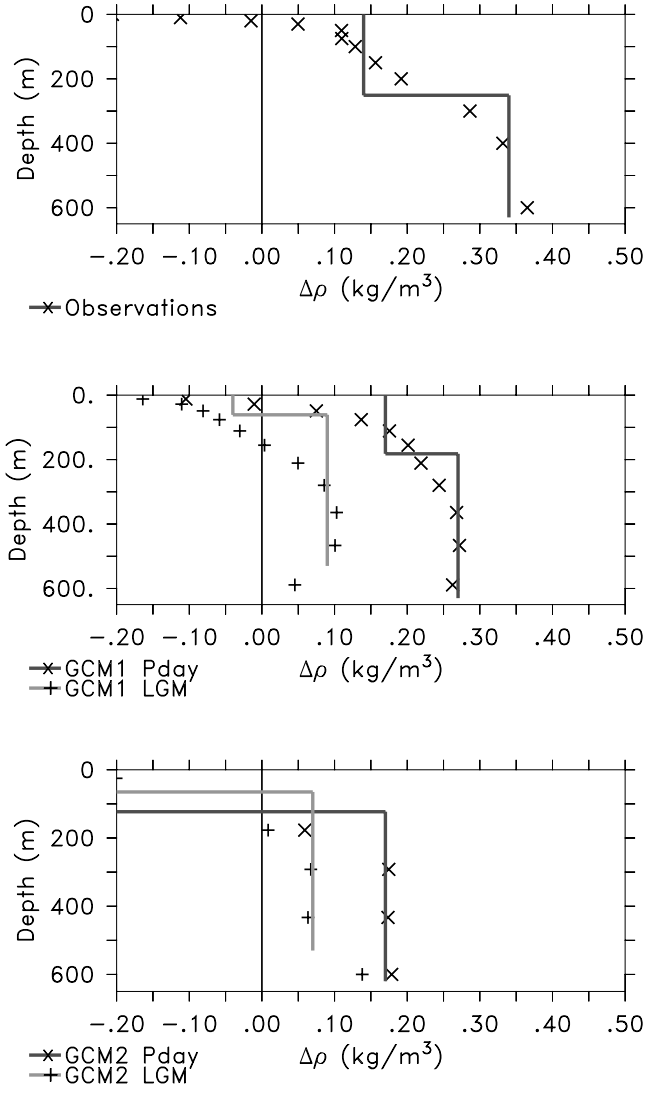

Figure 5. Across-strait density contrast from observations [*Levitus et al.*, 1994; *Levitus and Boyer*, 1994] and modeling (GCM1 is from *Paul and Schäfer-Neth* [2003] and GCM2 from *Meissner et al.* [2003]). The straight lines represent a two-layer model fit to the data for determining transport estimates.

Table 2. Density Contrast Across Denmark Strait Between Average North (30°W:20°W, 67°N:68°N) and South (30°W:25°W, 64°N:65°N) Profiles[a]

Data	Δρ	H_{eff}, m	Q, Sv
Observations[b]	0.34	370	1.7
GCM1[c]PD	0.27	497	1.6
GCM1-LGM	0.09	469	0.5
GCM2[d]PD	0.17	497	1.6
GCM2-LGM	0.07	465	0.3

[a]The transport follows from equation (1) where the sill depth is taken as 620 m for the present day 540 m for LGM.
[b]From *Levitus and Boyer* [1994] and *Levitus et al.* [1994].
[c]From *Paul and Schäfer-Neth* [2003].
[d]From *Meissner et al.* [2003].

[18] The hydraulically controlled transport through Denmark Strait depends not only on the effective height, but also on the density difference across the sill. Kösters (submitted manuscript, 2004) has shown for a broad range of density contrasts of $\Delta\rho = 0.16$ kg/m^3–0.72 kg/m^3 that the assumed linear relation of density contrast and transport ($Q \propto \Delta\rho$) holds.

4.2. LGM Density Contrast and Transport

[19] In order to assess possible LGM transports a rough estimate on the LGM density contrast was obtained from coarse-resolution global model data [*Paul and Schäfer-Neth*, 2003; *Meissner et al.*, 2003]. As mentioned before, the Greenland-Scotland Ridge topography is not properly resolved in these models, and hence the realistic simulation of water masses close to the Denmark Strait is limited. The average density contrast over the top 600 m for present-day conditions is slightly underestimated when compared to observations and will probably be underestimated for LGM conditions, too. We fitted two-layer models (by minimizing the error between two-layer model and data) to the observed and modeled Δρ values to obtain LGM transport estimates (Figure 5).

[20] The greatly reduced across-sill density difference would additionally diminish the hydraulic LGM transport by more than a factor of three (Table 2). A more reduced density contrast cannot be ruled out and a reduction by a factor of three is a conservative estimate consistent with different GCMs.

4.3. Descent of Overflow

[21] For the interpretation of paleoceanographic data derived from sediment cores it is important to know the path of the overflow. A common assumption in the literature seems to be that the overflow descent stayed more or less constant during the last glacial-interglacial cycle. This assumption is supported by the theoretical approach of *Killworth* [2001] who found from a force balance the overflow should descent at a constant rate of 250 m per 100 km pathway. This model is in contrast to observations [*Girton and Sanford*, 2003] and more complex stream-tube models [*Käse et al.*, 2003]. In the model the rate of descent $\frac{dz}{ds}$ is a function of bottom drag C_D, velocity v and overflow thickness H

$$\frac{dz}{ds} = \frac{C_D v^2}{g' H}. \tag{2}$$

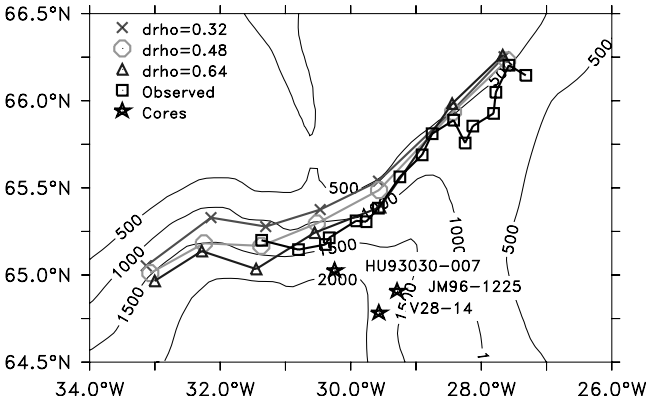

Figure 6. Descent of the overflow plume for different density contrasts ($\Delta\rho$ = 0.32, 0.48, 0.64 kg/m^3) compared with the observed overflow path (squares) [*Girton and Sanford*, 2003]. The stars denote core positions of paleoceanographic studies sampling the overflow (HU93030-007 from *Andrews et al.* [1998], JM96-1225 from *Hagen and Hald* [2002], and V28-14 from *Curry et al.* [1988]).

Even though the bottom has a strong influence on this balance we make the assumption that it was constant throughout time ($C_D = 10^{-3}$). However, we rather compare the path of the overflow for different density contrasts where high density contrasts resemble interglacial and low density contrast resemble stadial conditions.

[22] The path of the overflow is described as the position of the transport weighted center of gravity (COG) of the core of the overflow following *Girton and Sanford* [2003] as

$$COG = \frac{\int \Delta\rho\, v\, x\, dx}{\int \Delta\rho\, v\, dx}, \tag{3}$$

where x denotes the cross stream distance and v the along stream velocity. The position of the COG was then determined from the model results along the overflow path (Figure 6).

[23] The resulting overflow paths show that the position of the plume is sensitive to the density contrast. For a decreasing density contrast the speed of the plume is decreasing and the overflow position is shifted upward toward shallower depths. The sensitivity experiments were corroborated by the results from model GSR, where the overflow path for the LGM experiments was shifted to shallower depth as well (not shown).

5. Wind-Driven Transport (Experiment GSR)

[24] To achieve more realism we use in experiment GSR wind forcing and a mean but depth depending density profile instead of the two-layer setup as in DS. Experiments GSR-Ref A-D test the sensitivity to changes in surface stress for present-day conditions and experiments GSR-LGM A-D simulate the LGM overflow for different density profiles and wind stress (Table 3).

Table 3. Overview of Experiments With Average Density Profiles and Wind Forcing

Experiment	Time Slice, kyr BP	Buoyancy	Wind Stress
GSR-Ref-A	0	profile A[a]	none
GSR-Ref-B	0	profile A	ECMWF[b]
GSR-Ref-C	0	profile A	2 × ECMWF
GSR-Ref-D	0	profile A	4 × ECMWF
GSR-LGM-A	21.5	profile B[c]	none
GSR-LGM-B	21.5	profile B	AGCM[d]
GSR-LGM-C	21.5	profile C[e]	AGCM
GSR-LGM-D	21.5	profile B	AGCM2[f]

[a]Mean density profile from *Levitus et al.* [1994] and *Levitus and Boyer* [1994].
[b]Wind stress from *Gibson et al.* [1997].
[c]Mean density contrast from *Paul and Schäfer-Neth* [2003].
[d]Wind stress from *Paul and Schäfer-Neth* [2003].
[e]Mean density contrast from *Meissner et al.* [2003].
[f]Wind stress from *Lohmann and Lorenz* [2000].

[25] The surface stress for the present day was derived from the mean winter (DJF) wind field from the ECMWF climatology [*Gibson et al.*, 1997], which was scaled by factors 0, 1, 2 and 4 to test the sensitivity of the Greenland-Scotland Ridge volume exchange toward changes in the surface stress (Figure 7).

[26] In the case of no wind, the DSOW transport is solely buoyancy forced. We obtain 1.6 Sv DSOW transport with no wind which corresponds to the DS experiment with H_{eff} = 300 m. For increasing wind stress the transport is proportional increasing. The transport shows a linear response to the increase in wind forcing (Table 4).

[27] DSOW for the present day is commonly defined as more dense than 27.8. For the LGM we defined DSOW to be more dense than 28.7 which takes the global salinity change of the glacial into account. Experiments GSR-LGM show a strongly reduced transport of DSOW by a factor of

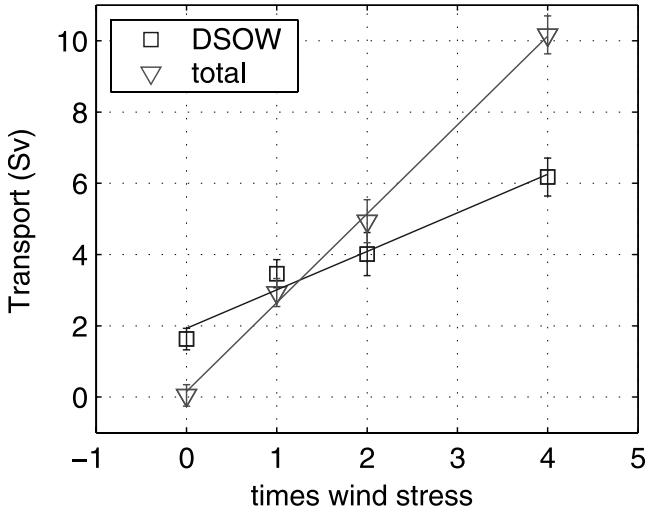

Figure 7. Relation between wind forcing and transport. The wind stress is the mean, present-day winter (DJF) surface stress as obtained from ECMWF, linearly scaled by the factor given at the x axis. DSOW is the transport of dense water and total stands for the depth-integrated (barotropic) transport.

Table 4. Volume Transport From the GSR-Ref Experiments With DSOW Being the Transport of Dense Water Only and Total is the Full Depth-Integrated Transport[a]

Experiment	Time Slice, kyr BP	DSOW, Sv	Total, Sv
GSR-Ref-A	0	1.6 ± 0.3	0.0 ± 0.3
GSR-Ref-B	0	3.5 ± 0.4	2.9 ± 0.4
GSR-Ref-C	0	4.0 ± 0.6	4.9 ± 0.5
GSR-Ref-D	0	6.2 ± 0.5	10.2 ± 0.6

[a]The error range indicates the 95% confidence bounds.

five during the LGM (Table 5). In case of no wind the transport ceases completely, for strong glacial wind conditions the overflow is still weakened by a at least a factor of 2.

[28] The total transport values through Denmark Strait show significant barotropic southward flow of up to 1.8 Sv even though the overflow is strongly reduced. This southward flow is primarily wind-driven. However, the robust results of these very different initial conditions and forcings is that the LGM overflow was significantly reduced most likely to less then 0.5 Sv.

6. Surface Cross-Ridge Exchange

[29] The dispersal of marine biota such as planktonic foraminifera is accomplished via passive advection. Here we used Lagrangian drifter to simulate the cross-ridge transport for glacial conditions. The GSR model was employed with mean density profiles and wind stress (GSR-REF A, GSR-LGM B). The resulting surface circulation and distribution of selected floats is shown in Figure 8.

[30] For modern conditions 17% of the surface drifters follow the Irminger current along the western Icelandic coast in harmony with the surface circulation scheme of *Hansen and Østerhus* [2000], whereas for glacial conditions the northward particle transport is significantly reduced to 2%. For glacial conditions our results suggest an additional northward transport to the east close to the Icelandic coast toward the north. Between 2 and 6% of the floats released east of Iceland circumvent Iceland in a cyclonic sense to the northwest. Hence subpolar planktic foraminifera found at the Northern Denmark Strait [*Völker*, 1999] do not necessarily indicate that there was an anticyclonic warm northward transport through Denmark Strait as for the present day but these specimen could have arrived there along the eastern Icelandic coast via the cyclonic route.

7. Discussion

[31] One of the aims of this study was to determine the maximum hydraulically controlled transport for deglacial and LGM conditions. Therefore we have shown that the transport estimates from the theoretical model of *Whitehead et al.* [1974] could be corroborated for the present day using a full three-dimensional numerical model. Not only that the modeling results compare well with observations in terms of volume transport and overflow path for the present day but we could establish that the same theory is in principle valid since the LGM. The ratio of modeled-to-theoretical transport in this study is about 0.5 ± 0.3 for the upstream area, which is lower than the values found by *Käse and Oschlies* [2000] (0.6). This is attributed to the different model setup, especially the upstream circulation. *Whitehead* [1998] used field data to asses the overflow strength and found a value of 0.8, which is the same as in our experiment GSR-REF B (not shown).

[32] Moreover, this is of interest for present-day conditions when considering the recent observations of a North Atlantic Deep Water density reduction [*Dickson et al.*, 2002]. From our findings that would be related to a decreasing overflow activity. These density variations are only small compared to the reduced density contrast found for the LGM.

[33] Our results suggest that hydraulic control can be used as a parameterization in coarse-resolution models. It was shown to work reliably for a fixed setup, giving some confidence in using this approach to improve the representation of the Denmark Strait Overflow in GCMs. For coarse-resolution models, the implication is that the Denmark Strait Overflow can in principle be represented by a hydraulic parameterization using a scaling factor. This scaling factor is probably influenced by the upstream circulation, as only recently shown [*Helfrich and Pratt*, 2003]. However, for fixed conditions, the simple hydraulic relation could be shown to be valid, which allows conclusions to be drawn about the influence of changing sill height and density contrasts under otherwise constant conditions. However, one must be aware that by choosing a scaling factor; assumptions about a fixed upstream circulation were made. This is obviously a restriction; but because of the poor performance of GCMs in this region; uncertainties related to the scaling factor pose a secondary problem. Unfortunately, the reduction of the density contrast for the LGM is uncertain; but different models show the same tendency of a greatly reduced contrast. Furthermore, the recent glacial SST reconstructions of *Pflaumann et al.* [2003], showing a greatly reduced gradient due to a southward shift of the polar front, support this view. Using these data the hydraulic theory predicted a ceased DSOW transport.

[34] A common assumption made inherent in many paleoceanographic studies seems to be that the position of the overflow core does not change from today's. From our examination of the overflow path we conclude that a core location close to the present-day overflow is not necessary close to the LGM overflow. Moreover if it shifted the position it would have been shallower. Therefore we point out that an appropriate coring location would be west of the

Table 5. Volume Transport From the GSR-LGM Experiments With DSOW Being the Transport of Dense Water Only and Total is the Full Depth-Integrated Transport

Experiment	Time Slice, kyr BP	DSOW, Sv	Total, Sv
GSR-LGM-A	21.5	0.0 ± 0.0	0.2 ± 0.0
GSR-LGM-B	21.5	0.7 ± 0.0	1.3 ± 0.0
GSR-LGM-C	21.5	0.0 ± 0.0	1.8 ± 0.1
GSR-LGM-D	21.5	0.4 ± 0.0	0.9 ± 0.0

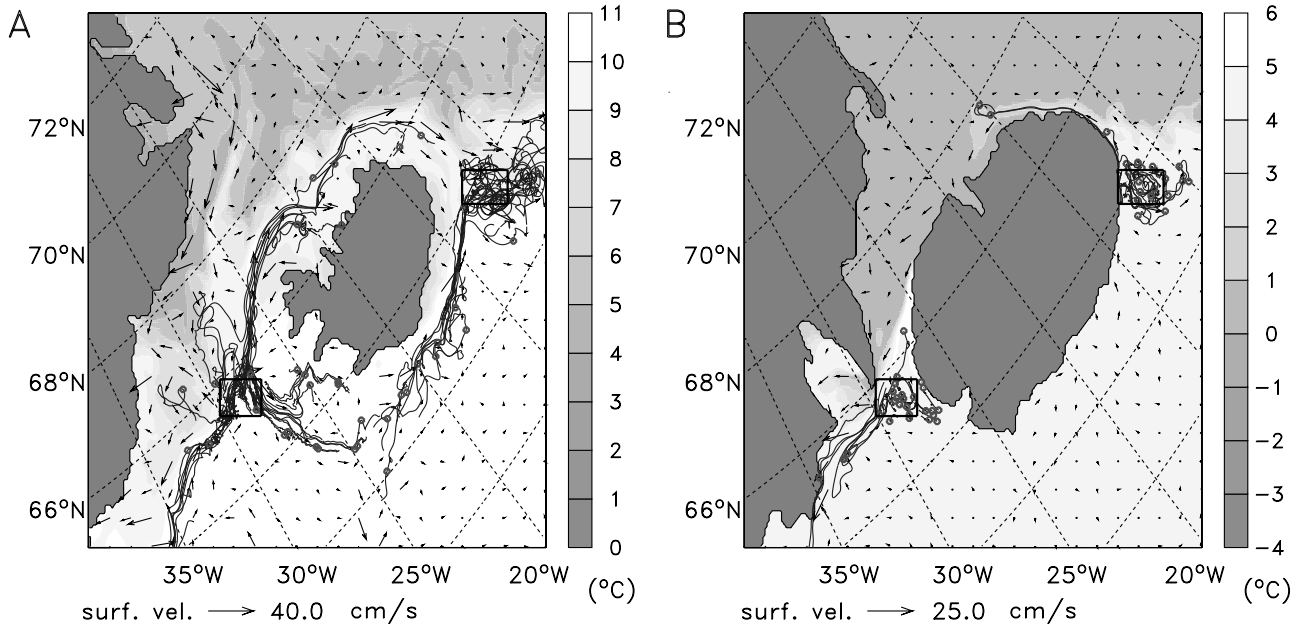

Figure 8. Surface temperature, circulation, and Lagrangian drifter pathways for (a) modern conditions from experiment GSR-Ref A and for (b) glacial conditions from experiment GSR-LGM B. See color version of this figure at back of this issue.

overflow not east of it as commonly done. We are aware that these recommendation is probably not easy to follow due to sedimentological aspects being more important, but it has to be taken into account when interpreting the data. Even though there will be influence of the DSO on cores located close to it by e.g., shedding eddies a significant contribution of the Irminger Current has to be assumed.

[35] Even though the hydraulic model of the first part gave good results for the present day and could be corroborated for deglacial times and the LGM it is not necessarily the most realistic estimate for the LGM. Generally an increased wind stress is found for the LGM [*Shin et al.*, 2003]. Therefore we investigated the influence of increased wind stress on the DSO. From average profiles and wind stress we find doubling of the DSOW transport when quadrupled the wind stress. Where the importance of this result for the present day is probably for climate change scenarios this shows that for the LGM the wind-driven circulation in the Denmark Strait was more important then today. This leaves the question why the measurements do not show variability at seasonal or interannual timescales if wind has an influence? Here, we point to other modeling studies where the overflow shows atmospheric signals such as the NAO [*Nilsen et al.*, 2003]. Owing to the limitation of the modeling domain, the missing annual cycle and the closed wall of the modeling domain we do not want to overemphasize these results. However, the consistent result of all experiments is a significantly reduced North Icelandic Irminger Current. The cyclonic circulation close to the Icelandic coast is not necessarily part of the North Atlantic Current but an effect of the changed LGM wind field. Obviously these modeling results depend on the prescribed wind stress, which might have been different from what we use, but our results may be support the reconstructed SSTs of *Hagen and Hald* [2002] showing an oscillating heat conveyor around Iceland. Another implication of the modeled surface circulation is that subpolar planktic foraminifera found at the Northern Denmark Strait [*Völker*, 1999] not necessarily indicate that there was a northward warm water transport through Denmark Strait but these specimen could have arrived there via the cyclonic route.

8. Conclusions

[36] We investigated the dense water transport through Denmark Strait for changing gateway depth and aperture, resembling present, deglacial and LGM bathymetries. The observed and maximum hydraulically predicted flow were compared and it was found that the theoretical values fit the observed ones when linearly scaled. We suggest a range in the scaling factor of hydraulic theory from 0.4 to 0.8, with 0.5 being a reasonable value for the parameterization when implemented into a GCM. Moreover, hydraulic control may also be a useful tool for estimating the LGM overflow strength from geological records, once density fields are resolved.

[37] Comparing the LGM and present-day results, the overflow was changed during the LGM due to the following factors.

[38] 1. A reduction of overflow strength due to a change in gateway depth and aperture arising from GIA, leading to a significant reduction in volume transport of ~33%.

[39] 2. A reduction in density contrast of more than 63% as suggested by a global model.

[40] 3. An increase of transport due to the increased glacial wind stress.

[41] 4. A shift to shallower depth by up to 500 m due to the changed force balance of the descending plume.

[42] We suggest that the Denmark Strait Overflow during the LGM was at least reduced by a factor of 5 from 3.5 Sv to 0.7 Sv. In addition to these effects the northward surface water transport with the Irminger Current through the Denmark Strait was reduced for the glacial circulation whereas there was increased surface water transport directly to the east of Iceland.

[43] **Acknowledgments.** We are grateful to Larry Peterson and two anonymous reviewers for helpful comments. We highly appreciate discussions and improvements of A. Schmittner and M. Schulz on the draft version of this document. We would also like to thank M. Sarnthein for helpful discussion and supervising the DFG funded project Ocean Gateways (http://www.passagen.uni-kiel.de).

References

Andrews, J. T., and S. Cartee-Schoolfield (2003), Late Quaternary lithofacies, provenance, and depositional environments (12–30 cal ka), north and south of the Denmark Strait, *Mar. Geol.*, *199*, 65–82.

Andrews, J. T., T. A. Cooper, A. E. Jennings, A. B. Stein, and H. Erlenkeuser (1998), Late Quaternary iceberg-rafted detritus events on the Denmark Strait-southeast Greenland continental slope (65°N): Related to North Atlantic Heinrich events?, *Mar. Geol.*, *149*, 211–228.

Bennike, O., and S. Björck (2002), Chronology of the last recession of the Greenland Ice Sheet, *J. Quat. Sci.*, *17*, 211–219.

Blindheim, J., V. Borovkov, B. Hansen, S. A. Malmberg, W. R. Turrell, and S. Østerhus (2000), Upper layer cooling and freshening in the Norwegian Sea in relation to atmospheric forcing, *Deep Sea Res. Part I*, *47*, 655–680.

Clark, P. U., and A. C. Mix (2002), Ice sheets and sea level of the Last Glacial Maximum, *Quat. Sci. Rev.*, *21*, 1–7.

Curry, W. B., J.-C. Duplessy, L. D. Labeyrie, and N. J. Shackleton (1988), Changes in the distribution of δ^{13}c of deep water σco_2 between the last glaciation and the holocene, *Paleoceanography*, *3*, 317–341.

Denton, G., and T. Hughes (Eds.) (1981), *The Last Great Ice Sheets*, John Wiley, Hoboken, N. J.

Dickson, B., I. Yashayaev, J. Meincke, B. Turrell, S. Dye, and J. Holfort (2002), Rapid freshening of the deep North Atlantic ocean over the past four decades, *Nature*, *416*, 832–837.

Elliot, M., L. Labeyrie, and J.-C. Duplessy (2002), Changes in North Atlantic deep-water formation associated with the Dansgaard-Oeschger temperature oscillations (60–10 ka), *Quat. Sci. Rev.*, *21*, 1153–1165.

Fleming, K., and K. Lambeck (2004), Constraints on the Greenland Ice Sheet since the Last Glacial maximum from sea-level observations and glacial rebound models, *Quat. Sci Rev.*, in press.

Funder, S., and L. Hansen (1996), The Greenland ice sheet—Model for its culmination and decay during and after the last glacial maximum, *Bull. Geol. Soc. Denmark*, *42*, 137–152.

Gibson, J. K., P. Kallberg, S. Uppala, A. Hernandez, A. Nomura, and E. Serrano (1997), ECMWF Reanalysis Project Report Series-1. ERA description, *Tech. Rep.*, Eur. Cent. for Med. Range Weather Forecast., Reading, UK.

Girton, J. B., and T. B. Sanford (2003), Descent and modification of the overflow plume in the Denmark Strait, *J. Phys. Oceanogr.*, *33*, 1351–1364.

Girton, J. B., T. B. Sanford, and R. H. Käse (2001), Synoptic sections of the Denmark Strait overflow, *Geophys. Res. Lett.*, *28*, 1619–1622.

Grootes, P. M., and M. Stuiver (1997), Oxygen 18/16 variability in Greenland snow and ice with 10−3- to 10+5-year time resolution, *J. Geophys. Res.*, *102*, 26,455–26,470.

Hagen, S., and M. Hald (2002), Variation in surface and deep water circulation in the Denmark Strait, North Atlantic, during marine isotope stages 3 and 2, *Paleoceanography*, *17*(4), 1061, doi:10.1029/2001PA000632.

Haidvogel, D. B., and A. Beckmann (1999), *Numerical Ocean Circulation Modeling*, *Ser. on Environ. Sci. and Manage.*, vol. 2, Imperial College Press, London.

Haidvogel, D. B., H. G. Arango, K. Hedstrom, A. Beckmann, P. Malanotte-Rizzoli, and A. F. Shchepetkin (2000), Model evaluation experiments in the North Atlantic basin: Simulations in nonlinear terrain-following coordinates, *Dyn. Atmos. Oceans*, *32*, 239–281.

Hansen, B., and S. Østerhus (2000), North Atlantic-Nordic Seas exchanges, *Prog. Oceanogr.*, *45*, 109–208.

Helfrich, K. R., and L. J. Pratt (2003), Rotating hydraulics and upstream basin circulation, *J. Phys. Oceanogr.*, *33*, 1651–1663.

Huybrechts, P. (2002), Sea-level changes at the LGM from ice-dynamic reconstructions of the Greenland and Antarctic ice sheets during the glacial cycles, *Quat. Sci. Rev.*, *21*, 203–231.

Ingolfsson, O., A. Lysa, S. Funder, P. Möller, and S. Björck (1994), Late Quaternary glacial history of the central west coast of Jameson Land, East Greenland, *Boreas*, *23*, 447–458.

Käse, R. H., and A. Oschlies (2000), Flow through Denmark Strait, *J. Geophys. Res.*, *105*, 28,527–28,546.

Käse, R. H., J. B. Girton, and T. B. Sanford (2003), Structure and variability of the Denmark Strait Overflow: Model and observations, *J. Geophys. Res.*, *108*(C6), 3181, doi:10.1029/2002JC001548.

Killworth, P. D. (2001), On the rate of descent of overflows, *J. Geophys. Res.*, *106*, 22,267–22,275.

Lambeck, K., C. Smither, and P. Johnston (1998), Sea-level change, glacial rebound and mantle viscosity for northern Europe, *Geophys. J. Int.*, *134*, 102–144.

Larsen, B. (1983), Structure and development of the Greenland-Scotland ridge, in *Geology of the Greenland-Iceland Ridge in the Denmark Strait*, pp. 425–444, Plenum, New York.

Levitus, S., and T. P. Boyer (1994), *World Ocean Atlas 1994*, vol. 4, *Temperature*, NOAA Natl. Environ. Satellite Data and Inf. Serv., Washington, D. C.

Levitus, S., R. Burgett, and T. P. Boyer (1994), *World Ocean Atlas 1994*, vol. 3, *Salinity*, NOAA Natl. Environ. Satellite Data and Inf. Serv., Washington, D. C.

Lohmann, G., and S. Lorenz (2000), On the hydrological cycle under paleoclimatic conditions as derived from AGCM simulations, *J. Geophys. Res.*, *105*, 17,417–17,436.

Matthiesen, S., and K. Haines (2003), A hydraulic box model study of the Mediterranean response to postglacial sea-level rise, *Paleoceanography*, *18*(4), 1084, doi:10.1029/2003PA000880.

Meissner, K. J., A. Schmittner, A. J. Weaver, and J. F. Adkins (2003), Ventilation of the North Atlantic Ocean during the Last Glacial Maximum: A comparison between simulated and observed radiocarbon ages, *Paleoceanography*, *18*(2), 1023, doi:10.1029/2002PA000762.

Mienert, J., J. T. Andrews, and J. D. Milliman (1992), The East Greenland continental margin (65°N) since the Last Deglaciation: Changes in seafloor properties and ocean circulation, *Mar. Geol.*, *106*, 217–238.

National Center for Atmospheric Research (NCAR) (1986), NGDC ETOPO5 global ocean depth and land elevation, 5-min, *Tech. Rep.*, Boulder, Colo.

Nikolopoulos, A., K. Borens, R. Hietala, and P. Lundberg (2003), Hydraulic estimates of Denmark Strait overflow, *J. Geophys. Res.*, *108*(C3), 3095, doi:10.1029/2001JC001283.

Nilsen, J. E., Y. Gao, H. Drange, T. Furevik, and M. Bentsen (2003), Simulated North Atlantic-Nordic Seas water mass exchanges in an isopycnic coordinate OGCM, *Geophys. Res. Lett.*, *30*(10), 1536, doi:10.1029/2002GL01659.

Nost, O. A., and P. E. Isachsen (2003), The large-scale time mean ocean circulation in the Nordic Seas and Artic Ocean estimated from simplified dynamics, *J. Mar. Res.*, *61*, 175–210.

Paul, A., and C. Schäfer-Neth (2003), Modeling the water masses of the Atlantic Ocean at the Last Glacial Maximum, *Paleoceanography*, *18*(3), 1058, doi:10.1029/2002PA000783.

Pflaumann, U., et al. (2003), Glacial North Atlantic: Sea-surface conditions reconstructed by GLAMAP 2000, *Paleoceanography*, *18*(3), 1065, doi:10.1029/2002PA000774.

Sarnthein, M., et al. (2001), Fundamental modes and abrupt changes in North Atlantic circulation and climate over the last 60 ky—Concepts, reconstructions and numerical modeling, in *The Northern North Atlantic: A Changing Environment*, edited by P. Schäfer et al., pp. 365–410, Springer Verlag, New York.

Saunders, P. M. (2001), Ocean circulation and climate, in *The Dense Northern Overflows*, pp. 401–417, Academic, San Diego, Calif.

Shchepetkin, A. F., and J. C. McWilliams (2004), The regional ocean modeling system: A split-explicit, free-surface, topography-following coordinates ocean model, *Ocean Modell.*, in press.

Shin, S.-I., Z. Liu, B. Otto-Bliesner, E. C. Brady, J. E. Kutzbach, and S. P. Harrison (2003), A Simulation of the Last Glacial Maximum climate using the NCAR-CCSM, *Clim. Dyn*., *20*, 127–151.

van Kreveld, S. A., M. Sarnthein, H. Erlenkeuser, P. Grootes, S. Jung, M. J. Nadeau,U. Pflaumann, and A. Voelker (2000), Potential links between surging ice sheets, circulation changes and the Dansgaard-Oeschger cycles in the Irminger Sea, 60–18 kyr, *Paleoceanography*, *15*, 425–442.

Völker, A. (1999), Zur Deutung der Dansgaard-Oeschger Ereignisse in ultra-hochauflsenden Sedimentprofilen aus dem Europäischen Nordmeer, Ph.D. thesis, Univ. of Kiel.

Whitehead, J. A. (1998), Topographic control of oceanic flows in deep passages and straits, *Rev. Geophys.*, *36*, 423–440.

Whitehead, J. A., A. Leetmaa, and R. A. Knox (1974), Rotating hydraulics of strait and sill flows, *Geophys. Fluid Dyn.*, *6*, 101–125.

Willebrand, J., B. Barnier, C. Böning, C. Dieterich, P. D. Killworth, C. Le Provost, Y. L. Jia, J. M. Molines, and A. L. New (2001), Circulation characteristics in three eddy-permitting models of the North Atlantic, *Prog. Oceanogr.*, *48*, 123–161.

K. Fleming and D. Wolf, GeoForschungsZentrum Potsdam, Telegrafenberg, D-14473 Potsdam, Germany.

R. Käse, Institut für Meereskunde, Universität Hamburg, Bundersstr. 53, D-20146 Hamburg, Germany.

F. Kösters, Institut für Geowissenschaften, Universität Kiel, Ludewig-Meyn-Str. 10, D-24118, Kiel, Germany. (koesters@passagen.uni-kiel.de)

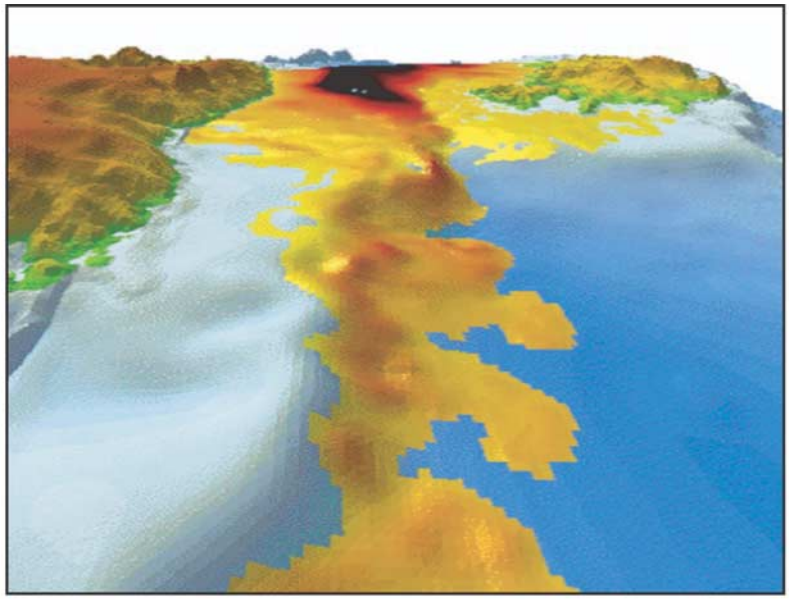

Figure 3. Snapshot of the descending overflow plume from the model experiments. Greenland is at the left, Iceland at the right margin. The shading of the overflow plume indicates the overflow thickness, with increasing thickness as darker gray and the full reservoir, as black, in the north.

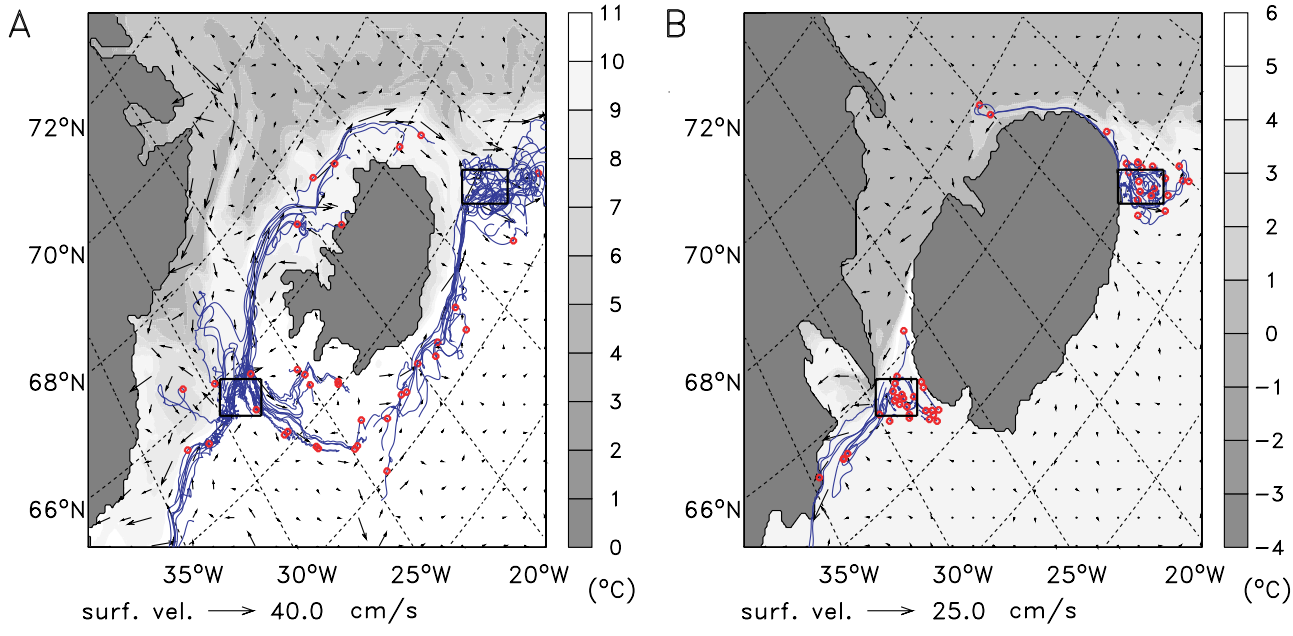

Figure 8. Surface temperature, circulation, and Lagrangian drifter pathways for (a) modern conditions from experiment GSR-Ref A and for (b) glacial conditions from experiment GSR-LGM B.